
Guided Adversarial Attack for Evaluating and Enhancing Adversarial Defenses

Gaurang Sriramanan*, Sravanti Addepalli*, Arya Baburaj, R.Venkatesh Babu
Video Analytics Lab, Department of Computational and Data Sciences
Indian Institute of Science, Bangalore, India

Abstract

Advances in the development of adversarial attacks have been fundamental to the progress of adversarial defense research. Efficient and effective attacks are crucial for reliable evaluation of defenses, and also for developing robust models. Adversarial attacks are often generated by maximizing standard losses such as the cross-entropy loss or maximum-margin loss within a constraint set using Projected Gradient Descent (PGD). In this work, we introduce a relaxation term to the standard loss, that finds more suitable gradient-directions, increases attack efficacy and leads to more efficient adversarial training. We propose *Guided Adversarial Margin Attack* (GAMA), which utilizes function mapping of the clean image to guide the generation of adversaries, thereby resulting in stronger attacks. We evaluate our attack against multiple defenses and show improved performance when compared to existing attacks. Further, we propose *Guided Adversarial Training* (GAT), which achieves state-of-the-art performance amongst single-step defenses by utilizing the proposed relaxation term for both attack generation and training.

1 Introduction

The remarkable success of Deep Learning algorithms has led to a surge in their adoption in a multitude of applications which influence our lives in numerous ways. This makes it imperative to understand their failure modes and develop reliable risk mitigation strategies. One of the biggest known threats to systems that deploy Deep Networks is their vulnerability to crafted imperceptible noise known as adversarial attacks, as demonstrated by Szegedy *et al.*[34] in 2014. This finding has spurred immense interest towards identifying methods to improve the robustness of deep neural networks against adversarial attacks. While initial attempts of improving robustness against adversarial attacks used just single-step adversaries for training [14], they were later shown to be ineffective against strong multi-step attacks by Kurakin *et al.*[23]. Some of the defenses introduced randomised or non-differentiable components, either in the pre-processing stage or in the network architecture, so as to minimise the effectiveness of generated gradients. However, many such defenses [4, 41, 33, 16] were later broken by Athalye *et al.*[3] using smooth approximations of the function during the backward pass or by computing reliable gradients using expectation over the randomized components. This game of building defenses against existing attacks, and developing attacks against the proposed defenses has been crucial for the progress in this field. Lately, the community has also recognized that the true testimony of a developed defense is to evaluate it against adaptive attacks which are constructed specifically to compromise the defense at hand [6].

Multi-step adversarial training is one of the best known methods of achieving robustness to adversarial attacks today [25, 43]. This training regime attempts to solve the minimax optimization problem of firstly generating strong adversarial samples by maximizing a loss, and subsequently training the

*Equal contribution.

Correspondence to: Gaurang Sriramanan <gaurangs@iisc.ac.in>, Sravanti Addepalli <sravantia@iisc.ac.in>

model to minimize loss on these adversarial samples. The effectiveness of the defense thus developed depends on the strength of the attack used for training. Therefore, development of stronger attacks is important for both evaluating existing defenses, and also for constructing adversarial samples during adversarial training. Indeed, the study of building robust adversarial defenses and strong adversarial attacks are closely coupled with each other today.

Adversarial attacks are constructed by maximizing standard losses such as cross-entropy loss or maximum-margin loss within a constrained set, as defined by the threat model. Due to the non-convex nature of the loss function, maximization of such a loss may not effectively find the path towards the class whose decision boundary is closest to the data point.

In this work, we aid the optimization process by utilizing the knowledge embedded in probability values corresponding to non-maximal classes to guide the generation of adversaries. Motivated by graduated optimization methods, we improve the optimization process by introducing an ℓ_2 relaxation term initially, and reducing the weight of this term gradually over the course of optimization, thereby making it equivalent to the primary objective towards the end. We demonstrate state-of-the-art results on multiple defenses and datasets using the proposed attack. We further analyse the impact of utilizing the proposed method to generate strong attacks for adversarial training. While use of the proposed attack for multi-step training shows only marginal improvement, we observe significant gains by using the proposed attack for single-step adversarial training. Single-step methods rely heavily on the initial gradient direction, and hence the proposed attack shows significant improvement over existing methods.

Our contributions in this work can be summarized as follows:

- We propose *Guided Adversarial Margin Attack* (GAMA), which achieves state-of-the-art performance across multiple defenses for a single attack and across multiple random restarts.
- We introduce a multi-targeted variant GAMA-MT, which achieves improved performance compared to methods that utilize multiple targeted attacks to improve attack strength [15].
- We demonstrate that Projected Gradient Descent based optimization (GAMA-PGD) leads to stronger attacks when a large number of steps (100) can be used, thereby making it suitable for defense evaluation; whereas, Frank-Wolfe based optimization (GAMA-FW) leads to stronger attacks when the number of steps used for attack are severely restricted (10), thereby making it useful for adversary generation during multi-step adversarial training.
- We propose *Guided Adversarial Training* (GAT), which achieves state-of-the-art results amongst existing single-step adversarial defenses. We demonstrate that the proposed defense can scale to large network sizes and to large scale datasets such as ImageNet-100.

Our code and pre-trained models are available here: <https://github.com/val-iisc/GAMA-GAT>.

2 Preliminaries

Notation: In this paper, we consider adversarial attacks in the setting of image classification using deep neural networks. We denote a sample image as $x \in \mathcal{X}$, and its corresponding label as $y \in \{1, \dots, N\}$, where \mathcal{X} indicates the sample space and N denotes the number of classes. Let $f_\theta : \mathcal{X} \rightarrow [0, 1]^N$ represent the deep neural network with parameters θ , that maps an input image x to its softmax output $f_\theta(x) = (f_\theta^1(x), \dots, f_\theta^N(x)) \in [0, 1]^N$. Further, let $C_\theta(x)$ represent the argmax over the softmax output. Thus, the network is said to successfully classify an image when $C_\theta(x) = y$. The cross-entropy loss for a data sample, (x_i, y_i) is denoted by $\ell_{CE}(f_\theta(x_i), y_i)$. We denote an adversarially modified counterpart of a clean image x as \tilde{x} .

Adversarial Threat Model: The goal of an adversary is to alter the clean input image x such that the attacked image \tilde{x} is perceptually similar to x , but causes the network to misclassify. Diverse operational frameworks have been developed to quantify perceptual similarity, and adversarial attacks corresponding to these constraints have been studied extensively. We primarily consider the standard setting of worst-case adversarial attacks, subject to ℓ_p -norm constraints. More precisely, we consider adversarial threats bound in ℓ_∞ norm: $\tilde{x} \in \{x' : \|x' - x\|_\infty \leq \varepsilon\}$.

While evaluating the proposed defense, we consider that the adversary has full access to the model architecture and parameters, since we consider the setting of worst-case robustness. Further, we assume that the adversary is cognizant of the defense techniques utilised during training or evaluation.

3 Related Works

3.1 Adversarial Attacks

A panoply of methods have been developed to craft adversarial perturbations under different sets of constraints. One of the earliest attacks specific to ℓ_∞ constrained adversaries was the Fast Gradient Sign Method (FGSM), introduced by Goodfellow *et al.* [14]. In this method, adversaries are generated using a single-step first-order approximation of the cross-entropy loss by performing simple gradient ascent. Kurakin *et al.* [22] introduced a significantly stronger, multi-step variant of this attack called Iterative FGSM (I-FGSM), where gradient ascent is iteratively performed with a small step-size, followed by re-projection to the constraint set. Madry *et al.* [25] developed a variant of this attack, which involves the addition of initial random noise to the clean image, and is commonly referred to as Projected Gradient Descent (PGD) attack.

Carlini and Wagner [5] explored the use of different surrogate loss functions and optimization methods to craft adversarial samples with high fidelity and small distortion with respect to the original image. The authors introduce the use of maximum margin loss for generation of stronger attacks, as opposed to the commonly used cross-entropy loss. Our proposed attack introduces a relaxation term in addition to the maximum margin loss in order to find more reliable gradient directions.

The Fast Adaptive Boundary (FAB) attack, introduced by Croce and Hein [9] produces minimally distorted adversarial perturbations with respect to different norm constraints, using a linearisation of the network followed by gradient steps which have a bias towards the original sample. While the FAB attack is often stronger than the standard PGD attack, it is computationally more intensive for the same number of iterations. Gowal *et al.* [15] introduced the Multi-Targeted attack, which cycles over all target classes, maximising the difference of logits corresponding to the true class and the target class. While this attack finds significantly stronger adversaries compared to PGD attack, it relies on cycling over multiple target classes, and hence requires a large computational budget to be effective. More recently, Croce and Hein [10] proposed AutoPGD, which is an automatised variant of the PGD attack, that uses a step-learning rate schedule adaptively based on the past progression of the optimization. They further introduce a new loss function, the Difference of Logits Ratio (DLR), which is a scale invariant version of the maximum margin loss on logits, and outperforms the ℓ_∞ based Carlini and Wagner (C&W) attack [5]. Additionally, they proposed AutoAttack, an ensemble of AutoPGD with the cross-entropy loss and the DLR loss, the FAB attack and Square attack [2], a score-based black-box attack which performs zeroth-order optimization.

3.2 Defenses Against Adversarial Attacks

With the exception of a few defenses [8, 1], most methods used to produce robust networks include some form of adversarial training, wherein training data samples are augmented with adversarial samples during training. Early works proposed training on FGSM [14], or Randomised FGSM (R-FGSM) [35] adversaries to produce robust networks. However, these models were still overwhelmingly susceptible to multi-step attacks [23] due to the Gradient Masking effect [27]. Madry *et al.* [25] proposed a min-max formulation for training adversarially robust models using empirical risk minimisation. It was identified that strong, multi-step adversaries such as Projected Gradient Descent (PGD), were required to sufficiently approximate the inner maximization step, so that the subsequent adversarial training yields robust models. Following this, Zhang *et al.* [43] presented a tight upper bound on the gap between natural and robust error, in order to quantify the trade-off between accuracy and robustness. Using the theory of classification calibrated losses, they develop TRADES, a multi-step gradient-based technique. However, methods such as TRADES and PGD-Training are computationally intensive, as they inherently depend upon the generation of strong adversaries through iterative attacks.

Consequently, efforts were made to develop techniques that accelerated adversarial training. Shafahi *et al.* [32] proposed a variant of PGD-training, known as Adversarial Training for Free (ATF), where the gradients accumulated in each step are used to simultaneously update the adversarial sample as well as network parameters, enabling the generation of strong adversaries during training, without additional computational overheads.

In order to mitigate gradient masking as seen in prior works that used single-step attacks for adversarial training, Vivek *et al.* [38] proposed the use of the R-MGM regularizer. The authors minimize the

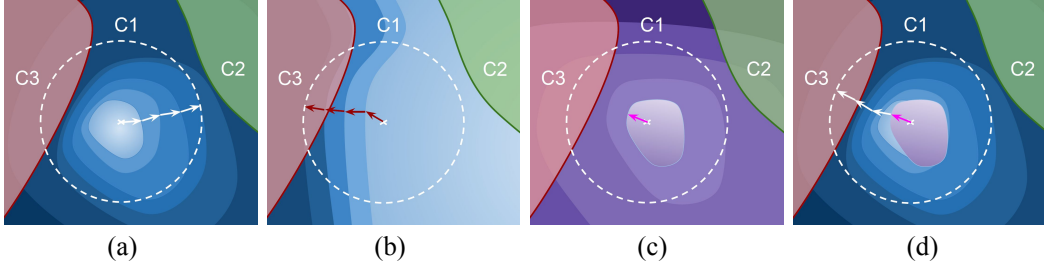


Figure 1: Schematic diagram of loss contours (a) Untargeted loss (b) Targeted loss w.r.t. class C3 (c) Guided loss for initial optimization (d) Path of adversary using GAMA

squared ℓ_2 norm of the difference between logits corresponding to FGSM and R-FGSM adversaries to train adversarially robust models. In contrast to this, we introduce a regularizer to minimize the squared ℓ_2 distance between the softmax outputs of clean and adversarial images, thereby improving the computational efficiency. Secondly, the adversary generation process uses the proposed Guided Adversarial Attack, thereby resulting in the use of a significantly stronger attack during training.

Contrary to prior wisdom, Wong *et al.* [40] (FBF), found the surprising result that R-FGSM training could indeed be successfully utilised to produce robust models. It was shown that R-FGSM adversarial training could be made effective with the use of small-step sizes for generation of adversaries, in combination with other techniques such as early-stopping and cyclic learning rates. With these techniques, they obtain better performance when compared to Adversarial Training for Free, with further reduction in computational requirements. While our proposed defense is also based on adversarial training with single-step adversaries, our choice of the loss function enables generation of stronger adversaries, thereby resulting in models that are significantly more robust. Further, we note that the acceleration techniques used in [40] can be utilized for our method as well.

4 Proposed Method

4.1 Impact of Initial Optimization Trajectory on Attack Efficacy

One of the most effective attacks known till date is the Projected Gradient Descent (PGD) attack [25], which starts with a random initialization and moves along the gradient direction to maximize cross entropy loss. Each iteration of PGD takes a step of a fixed size in the direction of sign of the gradient, after which the generated perturbation is projected back to the epsilon ball. Owing to the non-convex nature of the loss function, the initial gradient direction that maximizes cross-entropy loss may not lead to the optimal solution. This could lead to the given data sample being correctly classified, even if adversaries exist within an epsilon radius. This is shown in the schematic diagram of loss contours in Fig. 1(a), where the adversary moves towards class C2 based on the initial gradient direction, and fails to find the adversary that belongs to class C3.

This is partly mitigated by the addition of initial random noise, which increases the chance of the adversary moving towards different directions. However, this gain can be seen only when the attack is run for multiple random restarts, thereby increasing the computational budget required for finding an adversarial perturbation. Another existing approach that gives a better initial direction to the adversaries is the replacement of the standard untargeted attack with a combination of multiple targeted attacks [15]. This diversifies the initial direction of adversaries over multiple random restarts, thereby resulting in a stronger attack. This can be seen in Fig. 1(b), where the adversary is found by minimizing a targeted loss corresponding to the class C3, which has the closest decision boundary to the given sample. While this is a generic approach which can be used to strengthen any attack (including GAMA), it does not scale efficiently as the number of target classes increase.

In this paper, we propose to utilize supervision from the function mapping of clean samples in order to identify the initial direction that would lead to a stronger attack (Fig. 1(c)). The proposed attack achieves an effect similar to the multi-targeted attack without having to explicitly minimize the loss corresponding to each class individually (Fig. 1(d)). This leads to more reliable results in a single, or very few restarts of the attack, thereby improving the scalability of the attack to datasets with larger number of classes.

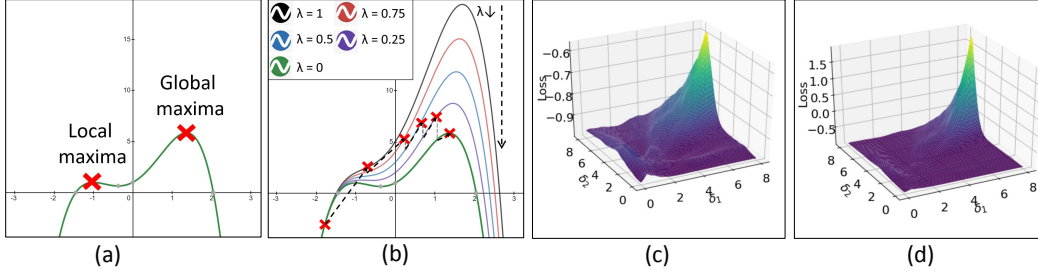


Figure 2: Addition of decaying ℓ_2 relaxation term for function smoothing and improved optimization (a) 1-D example showing maximization of the non-concave function, $1 - x(x-2)(x+1)(x+1)$ (b) The smoothed function after addition of ℓ_2 relaxation term is $1 - x(x-2)(x+1)(x+1) + \lambda(x+2)^2$. λ is reduced from 1 to 0 over iterations. Optimization trajectory is shown using black dotted lines and red cross marks. (c, d) Plot of the loss surface of an FGSM trained model on perturbed images of the form $x^* = x + \delta_1 g + \delta_2 g^\perp$, obtained by varying δ_1 and δ_2 . Here g is the sign of the gradient direction of the loss with respect to the clean image (x) and g^\perp is a direction orthogonal to g . Loss functions used are: (c) Maximum-margin loss, and (d) GAMA loss as shown in Eq.1, with λ set to 25. Addition of the relaxation term helps in smoothing the loss surface and suppressing gradient masking.

4.2 Guided Adversarial Margin Attack

Due to the inherent difficulty observed in the optimization of non-convex functions, several heuristic methods such as Graduated Optimization have been deployed to obtain solutions that sufficiently approximate global optima. To optimize a non-convex function, Graduated methods attempt to construct a family of smooth function approximations which are more amenable to standard optimization techniques. These function approximations are progressively refined in order to recover the original function toward the end of optimization. Hazan *et al.*[17] proposed to utilise projected gradient descent with a noisy gradient oracle, to optimize graduated function approximations obtained by local averaging over progressively shrinking norm balls. The authors characterise a family of functions for which their algorithm recovers approximate solutions of the global optima.

Along similar lines, we seek to introduce a relaxation term to obtain a series of smooth approximations of the primary objective function that is used to craft adversarial perturbations. We illustrate a simplified 1-dimensional example in Fig.2(a,b) to highlight the efficacy of graduated optimization through function smoothing. The loss function that is maximized for the generation of the proposed Guided Adversarial Margin Attack (GAMA) is as follows:

$$L = -f_\theta^y(\tilde{x}) + \max_{j \neq y} f_\theta^j(\tilde{x}) + \lambda \cdot \|\mathbf{f}_\theta(\tilde{x}) - \mathbf{f}_\theta(x)\|_2^2 \quad (1)$$

The first two terms in the loss correspond to the maximum margin loss in probability space, which is the difference between the probability score of the true class $f_\theta^y(x)$, and the probability score of the second most confident class $j \neq y$. The standard formulation of PGD attack maximizes cross-entropy loss for the generation of attacks. We use maximum-margin loss here, as it is known to generate stronger attacks when compared to cross-entropy loss [5, 15]. In addition to this, we introduce a relaxation term corresponding to the squared ℓ_2 distance between the probability vectors f_θ of the clean image x and the perturbed image \tilde{x} . This term is weighted by a factor λ as shown in Eq.1. Similar to graduated optimization, this weighting factor is linearly decayed to 0 over iterations, so that this term only aids in the optimization process, and does not disturb the optimal solution of the true maximum-margin objective. As shown in Fig.2(c,d), the ℓ_2 relaxation term indeed leads to a smoother loss surface in an FGSM trained model.

The gradients of this ℓ_2 relaxation term are a weighted combination of the gradients of each of the class confidence scores of the perturbed image. Each term is weighted by the difference in corresponding class confidence scores of the perturbed image and clean image. Therefore, a direction corresponding to the gradient of a given class confidence score is given higher importance if it has already deviated by a large amount from the initial class confidence of the clean image. Thus, the weighting of the current gradient direction considers the cumulative effect of the previous steps, bringing about an advantageous effect similar to that of momentum. This helps direct the initial

Algorithm 1 Guided Adversarial Margin Attack

```
1: Input: Network  $f_\theta$  with parameters  $\theta$ , Input image  $x$  with label  $y$ , Attack Size  $\varepsilon$ , Step-size  $\eta$  or  
   Convex parameter  $\gamma$ , Initial Weighting factor  $\lambda_0$ , Total Steps  $T$ , Relaxation Steps  $\tau$ , Learning  
   Rate Schedule  $S = \{t_1, \dots, t_k\}$ , Learning Rate Drop Factor  $d$   
2: Output: Adversarial Image  $\tilde{x}_T$   
3:  $\delta = \text{Bern}(-\varepsilon, \varepsilon)$  // Initialise Perturbation with Bernoulli Noise  
4:  $\tilde{x}_0 = x_0 = x + \delta, \lambda = \lambda_0$   
5: for  $t = 0$  to  $T - 1$  do  
6:    $L = \max_{j \neq y} \{f_\theta^j(\tilde{x}_t)\} - f_\theta^y(\tilde{x}_t) + \lambda \cdot \|f_\theta(\tilde{x}_t) - f_\theta(x_0)\|_2^2$   
7:    $\lambda = \max(\lambda - \lambda_0/\tau, 0)$   
8:   if mode == PGD then  
9:      $\delta = \delta + \eta \cdot \text{sign}(\nabla_\delta L)$   
10:     $\delta = \text{Clamp}(\delta, -\varepsilon, \varepsilon)$  // Project Back To Constraint Set  
11:   else if mode == FW then  
12:      $\delta = (1 - \gamma) \cdot \delta + \gamma \cdot \varepsilon \cdot \text{sign}(\nabla_\delta L)$   
13:   end if  
14:    $\tilde{x}_{t+1} = \text{Clamp}(x + \delta, 0, 1) - x$   
15:    $\tilde{x}_{t+1} = x + \delta$   
16:   if  $t \in S$  then  
17:      $\eta = \eta/d, \gamma = \gamma/d$   
18:   end if  
19: end for
```

perturbation more strongly towards the class which maximizes the corresponding class confidence, while also making the optimization more robust to spurious random deviations due to local gradients.

The algorithm for the proposed attack is presented in Algorithm-1. The attack is initialized using random Bernoulli noise of magnitude ε . This provides a better initialization when compared to Uniform or Gaussian noise, as the resultant image would be farther away from the clean image in this case when compared to other methods, resulting in more reliable gradients initially. Secondly, the space of all sign gradient directions is represented completely by the vertices of the ℓ_∞ hypercube of a fixed radius around the clean image, which is uniformly explored using Bernoulli noise initialization. The attack is generated using an iterative process that runs over T iterations, where the current step is denoted by t . At each step, the loss in Eq.1 is maximized to find the optimal \tilde{x} for the given iteration. The weighting factor λ of the ℓ_2 term in the loss function is linearly decayed to 0 over τ steps.

We propose two variants of the Guided Adversarial Margin Attack, GAMA-PGD and GAMA-FW. GAMA-PGD uses Projected Gradient Descent for optimization, while GAMA-FW uses the Frank-Wolfe [13] algorithm, also known as Conditional Gradient Descent. In PGD, the constrained optimization problem is solved by first posing the same as an unconstrained optimization problem, and further projecting the solution onto the constraint set. Gradient ascent is performed by computing the sign of the gradient, and taking step of size η , after which the perturbation is clamped between $-\varepsilon$ and ε , to project to the ℓ_∞ ball. On the other hand, the Frank-Wolfe algorithm finds the optimal solution in the constraint set by iteratively updating the current solution as a convex combination of the present perturbation and the point within the constraint set that maximises the inner-product with the gradient. For the setting of ℓ_∞ constraints, this point which maximises the inner-product is simply given by epsilon times the sign of the current gradient. Since the constraint set is convex, this process ensures that the generated solution lies within the set, and hence does not require a re-projection to the same. This process results in a faster convergence, thereby resulting in stronger attacks when the budget for the number of iterations is small. This makes GAMA-FW particularly useful in the setting of adversarial training, where there is a fixed budget on the number of steps used for attack generation. Finally the image is clamped to be in the range $[0, 1]$. We use an initial step size of η for GAMA-PGD and γ for GAMA-FW, and decay this by a factor of d at intermediate steps.

4.3 Guided Adversarial Training

In this section, we discuss details on the proposed defense GAT, which utilizes single-step adversaries generated using the proposed Guided Adversarial attack for training. As discussed in Section-4.2, the ℓ_2 term between the probability vectors of clean and adversarial samples in Eq.1 provides reliable gradients for the optimization, thereby yielding stronger attacks in a single run. The effectiveness and

Table 1: **Attacks (CIFAR-10)**: Accuracy (%) of various defenses (rows) against adversaries generated using different 100-step attacks (columns) under the ℓ_∞ bound with $\varepsilon = 8/255$. Architecture of each defense is described in the column "Model". WideResNet is denoted by W (W-28-10 represents WideResNet-28-10), ResNet-18 is denoted by RN18, Pre-Act-ResNet-18 is denoted by PA-RN18. ‡Additional data used for training, † $\varepsilon = 0.031$, *Defenses trained using single-step adversaries

	Model	Single run of the attack						5 random restarts				Top 5 targets	
		PGD	APGD	APGD	FAB	GAMA	GAMA	APGD	FAB	GAMA	GAMA	MT	GAMA
		100	CE	DLR		PGD	FW	DLR		PGD	FW		PGD-MT
Carmon <i>et al.</i> [7]‡	W-28-10	61.86	61.81	60.85	60.88	59.81	59.83	60.64	60.62	59.65	59.71	59.86	59.56
Schwag <i>et al.</i> [31]‡	W-28-10	59.93	59.61	58.39	58.29	57.51	57.50	58.26	58.06	57.37	57.38	57.48	57.20
Wang <i>et al.</i> [39]‡	RN18	52.87	52.38	49.70	48.50	48.12	48.17	49.37	48.33	47.92	47.97	47.76	47.58
Wang <i>et al.</i> [39]‡	W-28-10	62.63	61.76	58.98	57.53	57.19	57.14	58.56	57.29	56.84	56.92	56.80	56.54
Hendrycks <i>et al.</i> [19]‡	W-28-10	57.58	57.20	57.25	55.55	55.24	55.19	56.96	55.40	55.11	55.08	55.06	54.92
Rice <i>et al.</i> [29]	W-34-20	57.25	56.93	55.99	54.34	53.77	53.88	55.70	54.19	53.64	53.68	53.59	53.45
Zhang <i>et al.</i> [43]†	W-34-10	55.60	55.30	54.18	53.92	53.29	53.38	54.04	53.82	53.17	53.22	53.32	53.09
Madry <i>et al.</i> [25] [12]	RN-50	53.49	51.78	53.03	50.67	50.04	50.08	52.64	50.37	49.81	49.92	49.76	49.41
Wong <i>et al.</i> [40]*	PA-RN18	46.42	45.96	46.95	44.51	43.85	43.90	46.64	44.03	43.65	43.69	43.65	43.33
GAT (Ours)*	W-34-10	55.10	54.73	53.08	51.28	50.76	50.79	52.75	51.07	50.43	50.48	50.45	50.18

efficiency of the proposed attack make it suitable for use in adversarial training, to generate more robust defenses. This attack is notably more useful for training single-step defenses, where reliance on the initial direction is significantly higher when compared to multi-step attacks.

Initially, Bernoulli noise of magnitude α is added to the input image in order to overcome any possible gradient masking effect in the vicinity of the data sample. Next, an attack is generated by maximizing loss using single step optimization. We use the minimax formulation proposed by Madry *et al.*[25] for adversarial training, where the maximization of a given loss is used for the generation of attacks, and minimization of the same loss on the generated adversaries leads to improved robustness. In order to use the same loss for both attack generation and training, we use cross-entropy loss instead of the maximum-margin loss in Eq.1. This improves the training process, as cross-entropy loss is known to be a better objective for training when compared to maximum-margin loss. The generated perturbation is then projected onto the ε -ball. We introduce diversity in the generated adversaries by setting λ to 0 in alternate iterations, only for the attack generation. These adversarial samples (\tilde{x}_i) along with the clean samples (x_i) are used for adversarial training. The algorithm of the proposed single-step defense GAT is presented in detail in Algorithm-S1 of the Supplementary section.

Single-step adversarial training methods commonly suffer from gradient masking, which prevents the generation of strong adversaries, thereby leading to weaker defenses. The proposed training regime caters to the dual objective of minimizing loss on adversarial samples, while also explicitly enforcing function smoothing in the vicinity of each data sample (Details in Section-S1 of the Supplementary section). The latter outcome strengthens the credibility of the linearity assumption used during generation of single-step adversaries, thereby improving the efficacy of the same. This coupled with the use of stronger adversaries generated using GAMA enables GAT to achieve state-of-the-art robustness among the single-step training methods.

5 Experiments and Analysis

In this section, we present details related to the experiments conducted to validate our proposed approach. We first present the experimental results of the proposed attack GAMA, followed by details on evaluation of the proposed defense GAT. The primary dataset used for all our evaluations is CIFAR-10 [21]. We also show results on MNIST [24] and ImageNet [11] for the proposed attack GAMA in the main paper and for the proposed defense GAT in Section-S6 of the Supplementary. We use the constraint set given by the ℓ_∞ ball of radius $8/255$, $8/255$ and 0.3 for the CIFAR-10, ImageNet and MNIST datasets respectively. The implementation details of the proposed defense and attack are presented in Sections-S3 and S4 of the Supplementary.

5.1 Evaluation of the proposed attack (GAMA)

The performance of various defenses against different attack methods on CIFAR-10 dataset is shown in Table-1. We present results for both a single run of the attack (with a budget of 100 iterations), as well as the worst-case accuracy across 5 random restarts (with an effective budget of 5×100

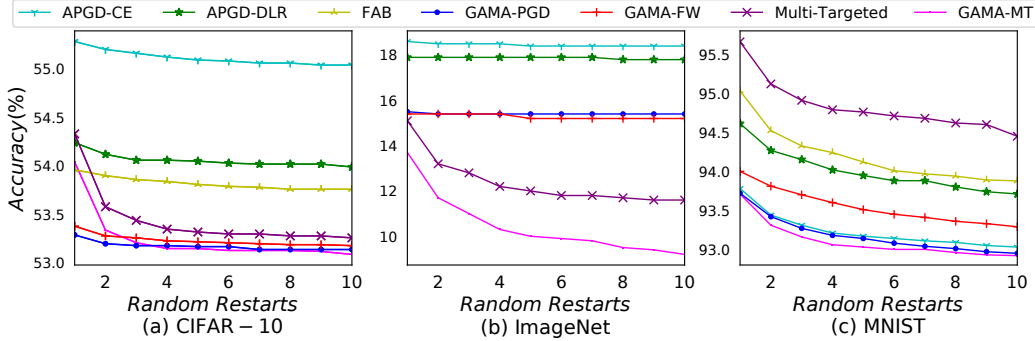


Figure 3: Accuracy (%) of different attacks against multiple random restarts. Evaluations are performed on TRADES WideResNet-34 model [43] for CIFAR-10, Madry *et al.*[12] ResNet-50 model for ImageNet (first 1000 samples), and TRADES SmallCNN [43] model for MNIST.

iterations). Notably, GAMA-PGD and GAMA-FW consistently outperform all other untargeted attacks across all defenses. Further, we remark that while the FAB attack stands as the runner-up method, it requires significantly more computation time, approximately 6 times that of GAMA-PGD and GAMA-FW.

The Multi-Targeted attack (MT) is performed by targeting the top 5 classes excluding the correct class. We present GAMA-MT, a multi-targeted version of the GAMA-PGD attack, where the maximum-margin loss is replaced by the margin loss targeted towards the top 5 classes excluding the true class. We note that the GAMA-MT attack is consistently the most effective attack across all defenses.

We further present evaluations on the TRADES WideResNet-34 model [43], PGD adversarially trained ResNet-50 model [25] and TRADES SmallCNN model [43] on the CIFAR-10, ImageNet (first 1000 samples) and MNIST datasets respectively against different attack methods in Fig.3. We find that while GAMA-PGD and GAMA-FW continue to consistently achieve the strongest attacks, they are also less sensitive to the random initialisation, when compared to other attack methods for varying number of random restarts. Thus the proposed attacks offer a more reliable bound on the robustness of models, within a single restart or very few restarts. The proposed multi-targeted attack GAMA-MT outperforms all other attacks significantly on ImageNet, and is marginally better than GAMA-PGD for CIFAR-10 and MNIST.

We evaluate the proposed attack on the TRADES leaderboard models [43]. A multi-targeted version of our attack GAMA on the WideResNet-34 CIFAR-10 model achieved the top position in the leaderboard, with 53.01% for a 100-step attack with 20 random restarts. On the SmallCNN MNIST model, we achieve an accuracy of 92.57% for a 100-step attack with 1000 random restarts.

Ablation Experiments: We present evaluations on the TRADES WideResNet-34 model on the CIFAR-10 test set with several ablations of the proposed attack in Table-S2 of the Supplementary section. We first observe that the maximum-margin loss is more effective when compared to the cross-entropy loss, for both 10 and 100 step attacks. Further, we observe that we obtain stronger adversaries while optimizing the margin loss between predicted probability scores, as compared to the corresponding logits. The weighting factor for the squared ℓ_2 relaxation term is linearly decreased to 0 for the 100-step attack, while it is kept constant for the 10-step attack. From the 100-step evaluations, we observe that the graduated optimization indeed aids in finding stronger adversaries. Further, the addition of initial Bernoulli random noise aids in improving 100-step adversaries. We also note that GAMA-FW achieves the strongest attack when the available budget on the number of steps for attack is relatively small.

5.2 Evaluation of the proposed defense (GAT)

The white-box accuracy of the proposed defense GAT is compared with existing defenses in Table-2. In addition to evaluation against standard attacks, we also report accuracy on the recently proposed ensemble of attacks called AutoAttack [10], which has been successful in bringing down the accuracy of many existing defenses by large margins. The existing single-step defenses are presented in the first partition of the table and the multi-step defenses are presented in the second. The proposed

Table 2: **Defenses (CIFAR-10)**: Accuracy (%) of different models (rows) against various ℓ_∞ norm bound ($\varepsilon = 8/255$, $\dagger\varepsilon = 0.031$) white-box attacks (columns). The first partition corresponds to single-step defenses, and the second has multi-step defenses. For the C&W attack, the mean ℓ_2 norm required to achieve high Fooling Rate (FR) is reported. Higher the ℓ_2 norm, better is the robustness.

Method	Model	Clean Acc (%)	Acc (%) on ℓ_∞ attacks						AA	C & W Mean ℓ_2
			FGSM	IFGSM 7-step	PGD (n-steps)			GAMA PGD-100		
					7	20	500			
Normal	RN18	92.30	15.98	0.00	0.00	0.00	0.00	0.00	0.00	0.108
FGSM-AT [14]	RN18	92.89	96.94	0.82	0.38	0.00	0.00	0.00	0.00	0.078
RFGSM-AT [35]	RN18	89.24	49.94	42.52	41.02	35.02	34.17	33.87	33.16	0.634
ATF [32]	RN18	71.77	46.67	45.06	44.96	43.53	43.52	40.34	40.22	0.669
FBF [40]	RN18	82.83	54.09	50.28	49.66	46.41	46.03	43.85	43.12	0.685
R-MGM [38]	RN18	82.29	55.04	50.87	50.03	46.23	45.79	44.06	43.72	0.745
GAT (Ours)	RN18	80.49	57.37	55.32	54.99	53.13	53.08	47.76	47.30	0.762
FBF [40]	WRN34	82.05	53.79	49.20	49.51	46.35	45.94	43.13	43.14	0.628
GAT (Ours)	WRN34	85.17	61.93	58.68	57.25	55.34	55.10	50.76	50.27	0.724
PGD-AT [25]	RN18	82.67	54.60	51.15	50.38	47.35	46.96	44.94	44.57	0.697
TRADES [43]	RN18	81.73	57.39	54.80	54.43	52.39	52.16	48.95	48.75	0.743
TR-GAT (Ours)	RN18	81.32	57.61	55.34	55.13	53.37	53.22	49.77	49.62	0.744
TRADES [43] \dagger	WRN34	84.92	61.06	58.47	58.09	55.79	55.56	53.29	53.18	0.705
TR-GAT (Ours)	WRN34	83.58	61.22	58.69	58.98	57.07	56.89	53.43	53.32	0.719

single-step defense GAT outperforms the current state-of-the-art single-step defense, FBF [40] on both ResNet-18 [18] and WideResNet-34-10 [42] models by a significant margin. In fact, we find that increasing model capacity does not result in an increase in robustness for FBF due to catastrophic overfitting. However, with the proposed GAT defense, we obtain a 2.97% increase in worst-case robust accuracy by using a larger capacity model, alongside a significant boost of 4.68% in clean accuracy. In addition to these results, the GAT WRN34-10 model is also evaluated against other state-of-the-art attacks, including our proposed attack GAMA in Table-1. Here, GAMA also serves as an adaptive attack to our defense, as the same loss formulation is used for both. We present evaluations on black-box attacks, gradient-free attacks, targeted attacks, untargeted attacks with random restarts and more adaptive attacks Section-S6 of the Supplementary. We also present all the necessary evaluations to ensure the absence of gradient masking [3] in the Supplementary material.

We further analyse the impact of using the proposed Guided Adversarial attack for adversary generation in the TRADES training algorithm. We utilize adversaries generated using GAMA-FW for this, as this algorithm generates stronger 10-step attacks when compared to others. Using this approach, we observe marginal improvement over TRADES accuracy. This improves further by replacing the standard adversaries used for TRADES training with GAMA-FW samples only in alternate iterations. We present results on the proposed 10-step defence TR-GAT using this combined approach in Table-2.

The improvement in robustness with the use of Guided Adversarial attack based adversaries during training is significantly larger in single-step adversarial training when compared to multi-step adversarial training. This is primarily because single-step adversarial training is limited by the strength of the adversaries used during training, while the current bottleneck in multi-step adversarial training methods is the amount of data available for training [7].

6 Conclusions

We propose Guided Adversarial Margin Attack (GAMA), which utilizes the function mapping of clean samples to guide the generation of adversaries, resulting in a stronger attack. We introduce an ℓ_2 relaxation term for smoothing the loss surface initially, and further reduce the weight of this term gradually over iterations for better optimization. We demonstrate that our attack is consistently stronger than existing attacks across multiple defenses. We further propose to use Frank-Wolfe optimization to achieve faster convergence in attack generation, which results in significantly stronger 10-step attacks. We utilize the adversaries thus generated to achieve an improvement over the current state-of-the-art adversarial training method TRADES. The proposed Guided Adversarial attack aids the initial steps of optimization significantly, thereby making it suitable for single-step adversarial training. We propose a single-step defense, Guided Adversarial Training (GAT) which uses the proposed ℓ_2 relaxation term for both attack generation and adversarial training, thereby achieving a significant improvement in robustness over existing single-step adversarial training methods.

7 Broader Impact

As Deep Networks see increasing utility in everyday life, it is essential to be cognizant of their worst-case performance and failure modes. Adversarial attacks in particular could have disastrous consequences for safety critical applications such as autonomous navigation, surveillance systems and medical diagnosis. In this paper, we propose a novel adversarial attack method, GAMA, that reliably bounds the worst-case performance of Deep Networks for a relatively small computational budget. We also introduce a complementary adversarial training mechanism, GAT, that produces adversarially robust models while utilising only single-step adversaries that are relatively cheap to generate. Thus, our work has immense potential to have a positive impact on society, by enabling the deployment of adversarially robust Deep Networks that can be trained with minimal computational overhead. During the development phase of systems that use Deep Networks, the GAMA attack can be used to provide reliable worst-case evaluations, helping ensure that systems behave as expected when deployed in real-world settings. On the negative side, a bad-actor could potentially use the proposed attack to compromise Deep Learning systems. However, since the proposed method is a white-box attack, it is applicable only when the entire network architecture and parameters are known to the adversary, which is a relatively rare scenario as model weights are often kept highly confidential in practice.

8 Acknowledgments and Disclosure of Funding

This work was supported by Uchhatar Avishkar Yojana (UAY) project (IISC_10), MHRD, Govt. of India. We would like to extend our gratitude to all the reviewers for their valuable suggestions.

References

- [1] S. Addepalli, B. S. Vivek, A. Baburaj, G. Sriramanan, and R. Venkatesh Babu. Towards Achieving Adversarial Robustness by Enforcing Feature Consistency Across Bit Planes. In *Proceedings of the IEEE Conference on Computer Vision and Pattern Recognition (CVPR)*, 2020. 3
- [2] M. Andriushchenko, F. Croce, N. Flammarion, and M. Hein. Square attack: a query-efficient black-box adversarial attack via random search. In *The European Conference on Computer Vision (ECCV)*, 2020. 3, 22
- [3] A. Athalye, N. Carlini, and D. Wagner. Obfuscated gradients give a false sense of security: Circumventing defenses to adversarial examples. In *International Conference on Machine Learning (ICML)*, 2018. 1, 9
- [4] J. Buckman, A. Roy, C. Raffel, and I. Goodfellow. Thermometer encoding: One hot way to resist adversarial examples. In *International Conference on Learning Representations (ICLR)*, 2018. 1
- [5] N. Carlini and D. Wagner. Towards evaluating the robustness of neural networks. In *IEEE Symposium on Security and Privacy (SP)*. IEEE, 2017. 3, 5, 17, 20
- [6] N. Carlini, A. Athalye, N. Papernot, W. Brendel, J. Rauber, D. Tsipras, I. Goodfellow, and A. Madry. On evaluating adversarial robustness. *arXiv preprint arXiv:1902.06705*, 2019. 1, 22
- [7] Y. Carmon, A. Raghunathan, L. Schmidt, J. C. Duchi, and P. S. Liang. Unlabeled data improves adversarial robustness. In *Advances in Neural Information Processing Systems (NeurIPS)*, 2019. 7, 9
- [8] J. Cohen, E. Rosenfeld, and Z. Kolter. Certified adversarial robustness via randomized smoothing. In *International Conference on Machine Learning (ICML)*, 2019. 3
- [9] F. Croce and M. Hein. Minimally distorted adversarial examples with a fast adaptive boundary attack. In *International Conference on Machine Learning (ICML)*, 2020. 3
- [10] F. Croce and M. Hein. Reliable evaluation of adversarial robustness with an ensemble of diverse parameter-free attacks. In *International Conference on Machine Learning (ICML)*, 2020. 3, 8, 18
- [11] J. Deng, W. Dong, R. Socher, L.-J. Li, K. Li, and L. Fei-Fei. ImageNet: A Large-Scale Hierarchical Image Database. In *Proceedings of the IEEE Conference on Computer Vision and Pattern Recognition (CVPR)*, 2009. 7, 14
- [12] L. Engstrom, A. Ilyas, H. Salman, S. Santurkar, and D. Tsipras. Robustness (python library), 2019. <https://github.com/MadryLab/robustness>. 7, 8

- [13] M. Frank and P. Wolfe. An algorithm for quadratic programming. *Naval research logistics quarterly*, 3 (1-2):95–110, 1956. 6
- [14] I. J. Goodfellow, J. Shlens, and C. Szegedy. Explaining and harnessing adversarial examples. In *International Conference on Learning Representations (ICLR)*, 2015. 1, 3, 9
- [15] S. Gowal, J. Uesato, C. Qin, P.-S. Huang, T. Mann, and P. Kohli. An alternative surrogate loss for pgd-based adversarial testing. *arXiv preprint arXiv:1910.09338*, 2019. 2, 3, 4, 5, 16, 17
- [16] C. Guo, M. Rana, M. Cisse, and L. van der Maaten. Countering adversarial images using input transformations. In *International Conference on Learning Representations (ICLR)*, 2018. 1
- [17] E. Hazan, K. Y. Levy, and S. Shalev-Shwartz. On graduated optimization for stochastic non-convex problems. In *International conference on machine learning (ICML)*, pages 1833–1841, 2016. 5
- [18] K. He, X. Zhang, S. Ren, and J. Sun. Deep residual learning for image recognition. In *Proceedings of the IEEE Conference on Computer Vision and Pattern Recognition (CVPR)*, 2016. 9, 14
- [19] D. Hendrycks, K. Lee, and M. Mazeika. Using pre-training can improve model robustness and uncertainty. In *International Conference on Machine Learning (ICML)*, 2019. 7
- [20] D. P. Kingma and J. Ba. Adam: A method for stochastic optimization. *arXiv preprint arXiv:1412.6980*, 2014. 18
- [21] A. Krizhevsky et al. Learning multiple layers of features from tiny images. 2009. 7, 14
- [22] A. Kurakin, I. Goodfellow, and S. Bengio. Adversarial examples in the physical world. *arXiv preprint arXiv:1607.02533*, 2016. 3
- [23] A. Kurakin, I. Goodfellow, and S. Bengio. Adversarial machine learning at scale. In *International Conference on Learning Representations (ICLR)*, 2017. 1, 3
- [24] Y. LeCun. The mnist database of handwritten digits. *Technical report*, 1998. 7, 14
- [25] A. Madry, A. Makelov, L. Schmidt, T. Dimitris, and A. Vladu. Towards deep learning models resistant to adversarial attacks. In *International Conference on Learning Representations (ICLR)*, 2018. 1, 3, 4, 7, 8, 9, 20, 21, 22
- [26] S.-M. Moosavi-Dezfooli, A. Fawzi, J. Uesato, and P. Frossard. Robustness via curvature regularization, and vice versa. In *Proceedings of the IEEE Conference on Computer Vision and Pattern Recognition (CVPR)*, 2019. 18
- [27] N. Papernot, P. McDaniel, I. Goodfellow, S. Jha, Z. B. Celik, and A. Swami. Practical black-box attacks against machine learning. In *Proceedings of the ACM Asia Conference on Computer and Communications Security (ACM ASIACCS)*, 2017. 3
- [28] C. Qin, J. Martens, S. Gowal, D. Krishnan, K. Dvijotham, A. Fawzi, S. De, R. Stanforth, and P. Kohli. Adversarial robustness through local linearization. In *Advances in Neural Information Processing Systems (NeurIPS)*, 2019. 18
- [29] L. Rice, E. Wong, and J. Z. Kolter. Overfitting in adversarially robust deep learning. In *International Conference on Machine Learning (ICML)*, 2020. 7
- [30] J. Rony, L. G. Hafemann, L. S. Oliveira, I. B. Ayed, R. Sabourin, and E. Granger. Decoupling direction and norm for efficient gradient-based l2 adversarial attacks and defenses. In *Proceedings of the IEEE Conference on Computer Vision and Pattern Recognition (CVPR)*, 2019. 20
- [31] V. Sehwal, S. Wang, P. Mittal, and S. Jana. Hydra: Pruning adversarially robust neural networks. In *Advances in Neural Information Processing Systems (NeurIPS)*, 2020. 7
- [32] A. Shafahi, M. Najibi, M. A. Ghiasi, Z. Xu, J. Dickerson, C. Studer, L. S. Davis, G. Taylor, and T. Goldstein. Adversarial training for free! In *Advances in Neural Information Processing Systems (NeurIPS)*, 2019. 3, 9
- [33] Y. Song, T. Kim, S. Nowozin, S. Ermon, and N. Kushman. Pixeldefend: Leveraging generative models to understand and defend against adversarial examples. In *International Conference on Learning Representations (ICLR)*, 2018. 1
- [34] C. Szegedy, W. Zaremba, I. Sutskever, J. Bruna, D. Erhan, I. J. Goodfellow, and R. Fergus. Intriguing properties of neural networks. In *International Conference on Learning Representations (ICLR)*, 2013. 1

- [35] F. Tramèr, A. Kurakin, N. Papernot, I. Goodfellow, D. Boneh, and P. McDaniel. Ensemble adversarial training: Attacks and defenses. In *International Conference on Learning Representations (ICLR)*, 2018. [3](#), [9](#), [15](#), [20](#), [21](#), [22](#)
- [36] D. Tsipras, S. Santurkar, L. Engstrom, A. Turner, and A. Madry. Robustness may be at odds with accuracy. In *International Conference on Learning Representations (ICLR)*, 2019. [13](#), [15](#)
- [37] J. Uesato, B. O’Donoghue, A. v. d. Oord, and P. Kohli. Adversarial risk and the dangers of evaluating against weak attacks. *arXiv preprint arXiv:1802.05666*, 2018. [22](#)
- [38] B. Vivek, A. Baburaj, and R. Venkatesh Babu. Regularizer to mitigate gradient masking effect during single-step adversarial training. In *Proceedings of the IEEE Conference on Computer Vision and Pattern Recognition (CVPR) Workshops*, 2019. [3](#), [9](#), [18](#), [20](#), [21](#), [22](#)
- [39] Y. Wang, D. Zou, J. Yi, J. Bailey, X. Ma, and Q. Gu. Improving adversarial robustness requires revisiting misclassified examples. In *International Conference on Learning Representations (ICLR)*, 2020. [7](#)
- [40] E. Wong, L. Rice, and J. Z. Kolter. Fast is better than free: Revisiting adversarial training. In *International Conference on Learning Representations (ICLR)*, 2020. [4](#), [7](#), [9](#), [18](#), [19](#), [20](#), [21](#), [22](#)
- [41] C. Xie, J. Wang, Z. Zhang, Z. Ren, and A. Yuille. Mitigating adversarial effects through randomization. In *International Conference on Learning Representations (ICLR)*, 2018. [1](#)
- [42] S. Zagoruyko and N. Komodakis. Wide residual networks. *arXiv preprint arXiv:1605.07146*, 2016. [9](#), [14](#)
- [43] H. Zhang, Y. Yu, J. Jiao, E. Xing, L. El Ghaoui, and M. I. Jordan. Theoretically principled trade-off between robustness and accuracy. In *International Conference on Machine Learning (ICML)*, 2019. [1](#), [3](#), [7](#), [8](#), [9](#), [16](#), [17](#), [20](#), [21](#), [22](#)

Supplementary Material

S1 Improved local properties induced by Guided Adversarial Training (GAT)

In this section, we present details on the improved local properties achieved using the proposed single-step defense, GAT (Guided Adversarial Training).

We examine the local properties of networks trained using the proposed methodology here. Formally, a function f is locally Lipschitz on a metric space \mathcal{X} , if for every $x \in \mathcal{X}$, there exists a neighborhood $U(x)$ such that f restricted to $U(x)$ is Lipschitz continuous, that is,

$$\|f(x) - f(y)\| \leq \mathcal{L} \cdot \|x - y\| \quad \forall y \in U(x) \quad (\text{S1})$$

In our framework, we consider \mathcal{X} to be the data-manifold, and f_θ as the softmax output of the neural network, where θ represents the parameters of the network. We first study the impact of the proposed squared ℓ_2 distance term in the loss function. Minimisation of this regularizer term leads to the following solution for θ^* :

$$\theta^* = \operatorname{argmin}_\theta \|f_\theta(x) - f_\theta(\tilde{x})\|_2^2 \quad (\text{S2})$$

where \tilde{x} is an adversary corresponding to clean image x . We note that the gradient of the loss on $f_\theta(x)$ represents the direction of steepest increase of the loss function. Thus, given that we want to obtain the strongest adversary achievable within a single backward-pass of the loss, we find \tilde{x} as given in Alg.S1, L6 to L9.

Since we want the network to be robust to adversaries lying within the ℓ_∞ -ball of radius ε centered at x , we ideally want a function f_{θ^*} that is locally Lipschitz within $U_\varepsilon(x)$:

$$U_\varepsilon(x) = \{x' : \|x - x'\|_\infty \leq \varepsilon\} \quad (\text{S3})$$

Given that $\|x - \tilde{x}\|_\infty \leq \varepsilon$, we have,

$$\|x - \tilde{x}\|_2 = \sqrt{\sum_{i=1}^d (x_i - \tilde{x}_i)^2} \leq \sqrt{\sum_{i=1}^d \varepsilon^2} \leq \sqrt{d} \cdot \varepsilon \quad (\text{S4})$$

where d is the dimension of the input space. For constrained adversaries, we now have,

$$\|f_{\theta^*}(x) - f_{\theta^*}(\tilde{x})\|_2 \leq \sqrt{d} \cdot \varepsilon \cdot \mathcal{L} \quad (\text{S5})$$

Thus, the prediction of f_{θ^*} is constant on $U_\varepsilon(x)$, if the Lipschitz constant \mathcal{L} is sufficiently small. Note that under this (strong) assumption, f_{θ^*} is *guaranteed* to be adversarially robust, as it predicts the same class for all images in the ε -constraint.

We note that the set \mathcal{X} is compact, since it is a closed and bounded subset of $[0, 1]^d$. Since the function f_θ is differentiable over \mathcal{X} , it is uniformly continuous over \mathcal{X} as well. Thus, there exists $\varepsilon' > 0$, such that prediction of f_θ is constant on $U_{\varepsilon'}(x)$ for all $x \in \mathcal{X}$. Thus, since adversarial perturbations cannot lie within an ε' -ball of any sample x , we are primarily interested in adversaries \tilde{x} such that:

$$\tilde{x} \in \mathcal{A}(x) = \{x' : \varepsilon' < \|x - x'\|_\infty \leq \varepsilon, f_\theta(x) \neq f_\theta(x')\} \quad (\text{S6})$$

Thus, the local Lipschitz constant \mathcal{L} of interest is given by:

$$\mathcal{L} = \sup_{\tilde{x} \in \mathcal{A}(x)} \frac{\|f_\theta(x) - f_\theta(\tilde{x})\|_2}{\|x - \tilde{x}\|_2} < \sup_{\tilde{x} \in \mathcal{A}(x)} \frac{1}{\sqrt{d} \cdot \varepsilon'} \|f_\theta(x) - f_\theta(\tilde{x})\|_2 \quad (\text{S7})$$

The square of the expression on the RHS is precisely the regularisation term used in the proposed loss function for training. Hence, imposing the proposed regularizer encourages the optimization procedure to produce a network that is locally Lipschitz continuous, with a smaller local Lipschitz constant. The actual optimisation procedure minimises the combined loss, with the first term given by the cross-entropy term, and the squared ℓ_2 loss term weighted by a factor λ . Note that without the inclusion of the first term, several degenerate solutions are possible, for example, a network that is constant for all images x . The value of λ determines the *effective* learning rate for the squared ℓ_2 loss term, and thus enforces the extent of function smoothness (refer Section-S3.2). The value of λ can be chosen so as to achieve the desired trade-off between clean accuracy and robustness [36]. For a fixed λ , we obtain a family of functions \mathcal{F}_λ that achieve the same cross-entropy loss. We can then extend the same analysis to f_{θ^*} which is the minimiser of the squared ℓ_2 loss term, and thus the combined total loss, amongst all functions $f_\theta \in \mathcal{F}_\lambda$.

Algorithm S1 Guided Adversarial Training

```
1: Input: Network  $f_\theta$  with parameters  $\theta$ , Training Data  $\mathcal{D} = \{(x_i, y_i)\}$ , Minibatch Size  $M$ , Attack Size  $\varepsilon$ , Initial Noise Magnitude  $\alpha$ , Epochs  $E$ , Learning Rate  $\eta$ 
2: for  $epoch = 1$  to  $E$  do
3:   for minibatch  $B_j \subset \mathcal{D}$  do
4:     Set  $L = 0$ 
5:     for  $i = 1$  to  $M$  do
6:        $\delta = \text{Bern}(-\alpha, \alpha)$ 
7:        $\delta = \delta + \varepsilon \cdot \text{sign}(\nabla_\delta (\ell_{CE}(f_\theta(x_i + \delta), y_i) + \lambda \cdot \|f_\theta(x_i + \delta) - f_\theta(x_i)\|_2^2))$ 
8:        $\delta = \text{Clamp}(\delta, -\varepsilon, \varepsilon)$ 
9:        $\tilde{x}_i = \text{Clamp}(x_i + \delta, 0, 1)$ 
10:       $L = L + \ell_{CE}(f_\theta(x_i), y_i) + \lambda \cdot \|f_\theta(\tilde{x}_i) - f_\theta(x_i)\|_2^2$ 
11:    end for
12:     $\theta = \theta - \frac{1}{M} \cdot \eta \cdot \nabla_\theta L$ 
13:  end for
14: end for
```

S2 Details on the datasets used

We run extensive evaluations on MNIST [24], CIFAR-10 [21] and ImageNet [11] datasets to validate our claims on the proposed attack and defense.

MNIST [24] is a handwritten digit recognition dataset consisting of 60,000 training images and 10,000 test images. The images are grayscale, and of dimension 28×28 . We split the training set into a random subset of 50,000 training images and 10,000 validation images.

CIFAR-10 [21] is a popular dataset in computer vision research, consisting of the following ten classes: Airplane, Automobile, Bird, Cat, Deer, Dog, Frog, Horse, Ship and Truck. The similarity of classes such as Cat and Dog make this a challenging dataset for the domain of adversarial robustness. The dimension of each image in this dataset is $32 \times 32 \times 3$. The original training set comprises of 50,000 images which we split into 49,000 training images and 1,000 validation images (equally balanced across all ten classes), while the test set has 10,000 images.

ImageNet [11] is a 1000-class dataset consisting of approximately 1.2 million training images and 50,000 images in the validation set. This dataset has a private test set which is not available for access to the public. Therefore, we use the designated validation set as the test set for our experiments. Furthermore, we split the designated training set into an 80-20 train-validation split. For training and evaluation of our proposed defense, we consider a random 100-class subset of this dataset, in order to ease the computation time and resource requirements. Even this subset is challenging due to the large dimensionality of the input space ($224 \times 224 \times 3$) and the high level of similarity between different classes. The set of 100 classes used for our experiments is shared along with our codes.

We use NVIDIA DGX workstation with V100 GPUs for our training and evaluations. The proposed single-step defense takes approximately 2 hours for training on ResNet-18 architecture for CIFAR-10 dataset. The proposed 100-step GAMA-PGD attack takes approximately 5 minutes for a single run to evaluate a ResNet-18 model on the CIFAR-10 test set.

S3 Details on Guided Adversarial Training

In this section, we present implementation details of the proposed defense.

S3.1 Architecture details

For evaluation of the proposed defense, we select a fixed architecture for each dataset, and use the same architecture to report results across all existing defense methods as well. We use a modified LeNet architecture with 4 convolutional layers as shown in Table-S1 for MNIST, and the ResNet-18 [18] architecture for our experiments on CIFAR-10 and ImageNet-100 datasets. We also report results on WideResNet-34-10 [42] architecture for the CIFAR-10 dataset with the proposed defense.

Table S1: Architecture used for MNIST dataset. Modified LeNet architecture is used for training robust models. We use the network, BB-MNIST as the source model for Black-Box attacks on the MNIST dataset

Modified LeNet (M-LeNet)	BB-MNIST
{conv(32,5,5) + Relu} \times 2	Conv(64,5,5) + Relu
MaxPool(2,2)	Conv(64,5,5) + Relu
{conv(64,5,5) + Relu} \times 2	Dropout(0.25)
MaxPool(2,2)	FC(128) + Relu
FC(512) + Relu	Dropout(0.5)
FC + Softmax	FC + Softmax

S3.2 Details on the training algorithm

The training algorithm for the proposed single-step defense GAT is presented in Algorithm-S1. This is explained in Section-4.3 of the main paper. In the proposed defense GAT, we first add Bernoulli noise of magnitude α to the clean image. We set the value of α to be either ε or $\varepsilon/2$ [35]. In the next step, we generate a GA-CE (Guided Adversarial Cross-Entropy) attack on the noise-added image, and finally project the generated perturbation onto the ε -ball of the clean image. In standard single-step adversarial training [35], the FGSM attack is of magnitude $(\varepsilon - \alpha)$. So, the perturbation is always within the ℓ_∞ ε -ball of the clean image and thus there is no need to project it back to the ε -ball. The proposed formulation however, can move the adversary outside the ε -ball thereby increasing the likelihood of the adversary lying on the boundary of the ε -ball after projection. In principle, this broader class of adversaries should lead to a stronger attack, since most of the adversaries are farther away from the original image when compared to a standard R-FGSM attack.

The two losses in the proposed framework (Alg.S1, L7,10) are combined by weighting the squared ℓ_2 loss term by a factor λ . This weighting term determines the trade-off between accuracy and robustness [36] as shown in Fig.S1(b). We observe that during the initial stages of training, the loss surface is relatively smooth, thereby requiring a low value for λ . This factor is stepped up towards the end of training. The learning-rate is decayed when the loss begins to plateau. We generally observe that for the first learning-rate update, both clean and adversarial accuracy improve in tandem if λ is kept fixed. As training progresses, the loss surface becomes increasingly convoluted; we thus step-up λ along with the subsequent decay in learning rate, so as to strike a balance between clean accuracy and adversarial robustness.

The λ step-up factor can be viewed as an effective learning rate increase for the squared ℓ_2 loss term. During adversarial training involving step learning rate decay, accuracy is boosted significantly for the initial few step decays. This results in a change in loss landscape, leading to an increase in loss on adversarial samples, as can be seen in case of R-FGSM training and PGD training in Fig. S2 (a and b). The training on adversarial samples is however unable to compensate for the increase in loss as the learning rate is too low. Thus, inclusion of the step-up factor ensures that the adversarial loss does not increase rapidly over epochs. It can be seen in Fig.S2 (d) that a combination of the proposed learning rate schedule and step-up factor is able to prevent an increase in loss. Similar to TRADES, the loss on clean and adversarial samples consistently reduces over epochs in the proposed method. It is also worth noting that the loss on FGSM samples is very close to the loss on PGD samples, thereby proving the effectiveness of training with single-step adversaries generated using the Guided Adversarial attack.

S3.3 Implementation details

GAT (Single-step defense): Before generating the attack for adversarial training in GAT defense, we add initial noise of magnitude ε for MNIST, and $\varepsilon/2$ for the other datasets. For the CIFAR-10 dataset, we use an initial λ and step-up factor of 10 and 4 respectively for ResNet-18 training, and 3 and 20 respectively for WideResNet-34-10 training. The same values of λ and step-up factor are used for both generation of attack (Alg.S1, L7) and training (Alg.S1, L10). We use the SGD optimizer with momentum of 0.9 and weight decay of $5e-4$ for all our experiments. The learning rate is set to 0.1 and decayed by a factor of 10, at epochs 70 and 85 for ResNet-18 and at epochs 55,70 and 75 for WideResNet-34-10. As discussed in Section-S3.2, the second learning rate update is accompanied by a λ step-up. The impact of variation in λ and λ step-up factor is shown in Fig.S1(b) and Fig.S1(c) respectively. It can be observed that the clean accuracy and accuracy on GAMA-PGD adversarial samples is stable across variations in the hyperparameters. As λ increases, there is a reduction in clean accuracy and an increase in robustness. This trend continues till a value of 10, after which the adversarial accuracy remains constant or starts reducing. We therefore select 10 as the optimum value. A similar trend is observed for variation in λ step-up factor as well. The slight reduction in robustness at high values of λ or λ step-up factor is due to the reduction in clean accuracy. Since accuracy on clean samples is an upper bound on adversarial robustness, over-regularization causes both to reduce.

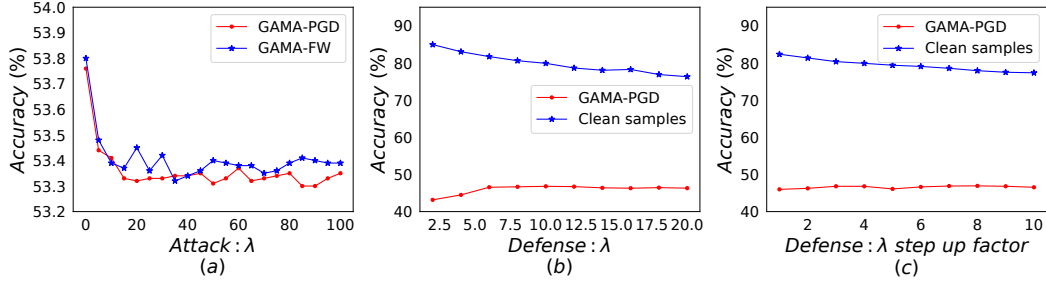


Figure S1: (a) Accuracy (%) of the TRADES-WRN34 model [43] trained on CIFAR-10 dataset, against the proposed GAMA-PGD and GAMA-FW attacks, across various settings of λ in Eq.1 of the main paper. This is the weight of ℓ_2 relaxation term in the loss. (b, c) Accuracy (%) of the proposed GAT defense on ResNet-18 models trained on CIFAR-10 dataset, across variation in hyperparameters used for the defense. λ (Alg.-S1, L7, 10) is varied in (b) and λ step up factor is varied in (c). Accuracy (%) on clean samples and 100-step GAMA-PGD adversaries is shown. GAMA-PGD attack settings are fixed to optimal values.

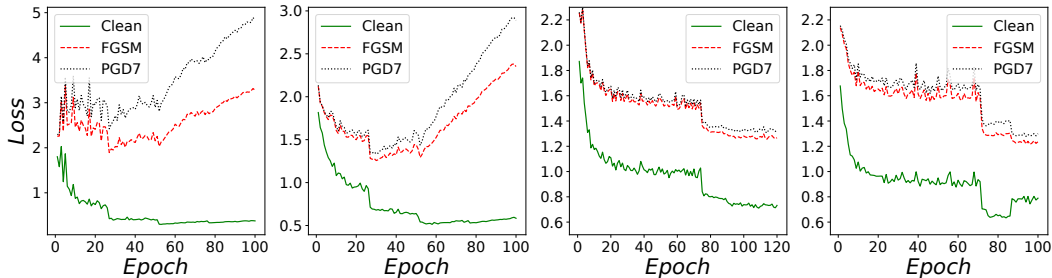


Figure S2: Plot of Cross-Entropy loss on CIFAR-10 test samples across epochs for different training methods: (a) R-FGSM-AT (b) PGD-AT (c) TRADES (d) GAT (Ours)

For ImageNet-100, we use an initial λ of 20 and step it up by a factor of 7 at epoch 90. The learning rate is 0.1 initially and decayed by a factor of 10 at epochs 60 and 90.

For MNIST, the initial learning rate is set to 0.01, and further decayed by a factor of 5 three times at regular intervals. In MNIST dataset, the clean accuracy shoots up to above 90% within the first epoch, and reaches a very high value in a few epochs. Hence, we do not need a simple drop in learning rate without λ step-up, for a further increase in robust accuracy. We therefore include the λ step-up factor at all three times of learning rate update. We set the value of λ to 15 and the λ step-up factor to 3.

We train our MNIST model for 50 epochs, CIFAR-10 model for 100 epochs and ImageNet-100 model for 120 epochs. The other methods are trained until convergence.

TR-GAT (Multi-step defense): We next present details on the proposed multi-step defense TR-GAT. To incorporate Guided Adversarial Attacks for TRADES training as shown in Table-2 in the main paper, we alternate between a 10-step PGD attack that maximises KL-Divergence and a 10-step GAMA-FW attack with a constant λ , set to the same value as the weighting used for the KL-Divergence term in training. We set this weighting term (called β in the original TRADES paper [43]) to be 5 and 6 respectively for the ResNet-18 and WideResNet-34 models on CIFAR-10 dataset. For training the TR-GAT model, we use the same learning rate schedule and total epochs as used for the corresponding TRADES model.

S4 Implementation details of the Guided Adversarial Margin Attack

The loss function that is maximized for generation of our proposed attack GAMA is shown in Eq.1 of the main paper. This consists of two terms, maximum margin loss and squared ℓ_2 relaxation term between the softmax vectors of clean and perturbed images. The squared ℓ_2 term is weighted by a factor λ , which is decayed to 0 over a fixed number of iterations. We set λ to 50 and decay this to 0 over 25 iterations. This aids the optimization process by providing a better initial direction. As shown in Fig.S1(a), the attack strength is stable over a wide range of λ values.

Prior to the attack generation, we add Bernoulli noise of magnitude ε to the image. Analogous to the training of Deep Neural Networks, generation of standard attacks are also known to benefit with a step learning rate schedule over the optimization process [15]. For the GAMA-PGD attack, we use an initial step size of $2 \cdot \varepsilon$

Table S2: **Ablations (CIFAR-10)**: Accuracy (%) of various attacks (rows) on TRADES-WRN34 [43] model under the ℓ_∞ bound with $\varepsilon = 0.031$, across different settings of number of steps and restarts.

Attacks	100 - step attacks		10 - step attacks	
	Single run	5 restarts	Single run	5 restarts
PGD (Cross-entropy loss)	55.61	55.27	56.7	56.31
PGD (Margin loss in logits space)	54.19	54.07	55.04	54.75
PGD (Margin loss in prob. space)	53.94	53.8	54.87	54.68
PGD (Margin loss and ℓ_2 loss in prob. space)	53.73	53.54	54.96	54.67
GAMA - PGD	53.29	53.17	54.95	54.66
GAMA - FW	53.38	53.22	54.27	54.00

and decay it by a factor of 10 at iterations 60 and 85 for a 100-step schedule. Similarly, for the GAMA-FW attack, we use an initial γ of 0.5 and decay it by a factor of 5 at the same iterations. For evaluating the TRADES leaderboard [43] WideResNet-34 CIFAR-10 model, we use a multi-targeted version of our attack; we run the attack for 100 steps, and 20 random restarts, wherein we alternate between the proposed GAMA loss and the margin loss corresponding to different classes over multiple restarts.

As noted by Gowal et al. [15], the loss surface of models adversarially trained on the MNIST datasets is complex. This necessitates different attack settings for this dataset. The threat model considered typically for MNIST is $\varepsilon = 0.3$. We set the initial λ to 5 and decay it to 0 in 50 iterations. For GAMA-PGD, we use an initial step size of ε and decay it by 10 at iterations 50 and 75. For GAMA-FW, γ of 0.5 is used initially and decayed by a factor of 5 at the same iterations.

S5 Details on Evaluation of the proposed attack

For evaluation of the proposed attacks (Table-1 and Fig.3 of the main paper, Fig.S1(a) of the supplementary), we use pre-trained models shared by the respective authors of various defenses. Therefore, the architecture of different models would be as chosen by the respective authors, and is thus not consistent across all defenses presented in Table-1 of the main paper.

S5.1 Ablation Experiments

We present evaluations on the TRADES WideResNet-34 model on the CIFAR-10 test set with several ablations of the proposed attack in Table-S2. We first observe that the maximum-margin loss, which is similar to the C&W ℓ_∞ based attack [5], is more effective when compared to the cross-entropy loss, for both 10 and 100 step attacks. Further, we observe that we obtain stronger adversaries while optimising the margin loss between predicted probability scores, as compared to the corresponding logits. The weighting factor for the squared ℓ_2 relaxation term is linearly decreased to 0 for the 100-step attack, while it is kept constant for the 10-step attack. From the 100-step evaluations, we observe that graduated optimisation indeed aids in finding stronger adversaries. Further, the addition of initial Bernoulli random noise aids in improving 100-step adversaries. We also note that GAMA-FW achieves the strongest attack when the available budget on the number of steps for attack is relatively small, making it suitable for use in multi-step adversarial training.

S5.2 Variation of Accuracy and Cross-Entropy loss across attack iterations

In Fig.S3, we plot the accuracy and Cross-Entropy loss across attack iterations for the TRADES ResNet-18 model on the CIFAR-10 dataset. The GAMA attack achieves lower accuracy and higher Cross-Entropy loss during the course of optimization, as compared to the attack generated using only the maximum-margin loss. We note from Fig.S3(b) that the decay of ℓ_2 relaxation term over the first 25 iterations in GAMA is crucial to allow Cross-Entropy loss to increase. Therefore, while the ℓ_2 relaxation term gives the right initialization, switching to the true maximum-margin optimization objective is important for achieving a stronger attack. We thus observe that the additional ℓ_2 relaxation term with a decaying coefficient indeed aids in the optimization process, and prevents the attack from stalling at points where the primary objective function attains a local maximum. Lastly, although the loss tends to oscillate before the first drop in step-size at iteration 60, we find that it is important to allow the attack to adequately explore the constraint set, in order to identify strong adversarial perturbations towards the end of optimization.

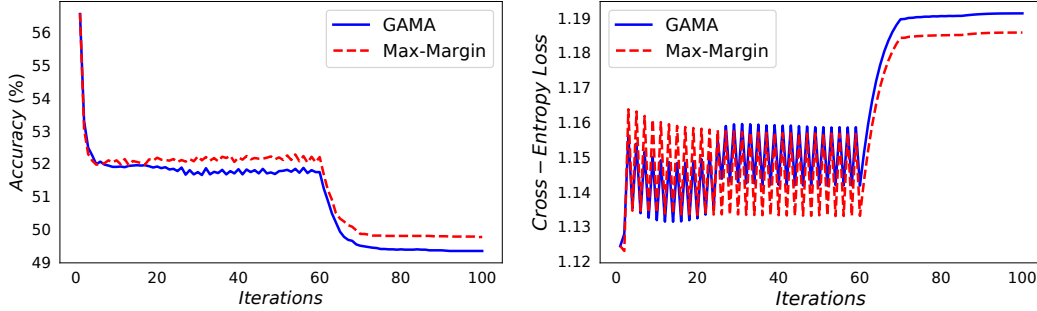


Figure S3: **Variation of Accuracy and Cross-Entropy Loss across attack iterations:** Plot of the Accuracy and Cross-Entropy Loss across attack iterations for the TRADES ResNet-18 defense, trained on the CIFAR-10 dataset. The proposed attack GAMA (Maximum-margin + ℓ_2 relaxation term) has been compared with a standard maximum-margin based attack.

Table S3: **GAT Ablations (CIFAR-10):** Accuracy (%) of various ablations of the GAT defense (rows) trained on ResNet-18 model under the ℓ_∞ threat model of $\varepsilon = 8/255$.

Ablations	Clean	PGD-100	AA
GAT (Proposed method)	80.49	53.08	47.30
A1: GAT, without alternating between CE and GA-CE attacks	80.22	51.50	46.52
A2: GAMA max-margin loss for attack and training	23.22	15.64	10.98
A3: GA-CE attack + standard defense (training on $CE_{clean} + CE_{adv}$)	90.21	33.57	32.29
A4: Standard attack + standard defense (R-FGSM training)	89.24	34.23	33.16
A5: Standard (CE) attack + GAT defense	80.05	51.8	44.21

S5.3 Use of ADAM optimizer in the GAMA attack

We also implement an ablation of the proposed GAMA-PGD attack using the ADAM optimizer [20] with the true gradients, instead of using Stochastic Gradient Descent with signed gradients. We perform a hyperparameter search over the initial step-size, step-schedule and decaying coefficient of the ℓ_2 smoothing term. We find that the attack is marginally weaker when the ADAM optimizer is used; the strongest 100-step attack obtained over the entire hyperparameter search achieves 53.66% accuracy on the TRADES WideResNet-34 model for a single run of the attack, compared to 53.29% as obtained by the original GAMA-PGD attack.

S6 Details on Evaluation of the proposed defense

In this section, we present additional experimental results to support our claims on the proposed single-step defense GAT. For CIFAR-10 dataset, we report results on ResNet-18 and WideResNet-34-10 architectures for the proposed method in the main paper. We note that while defense methods such as CURE [26] and 2-step LLR [28] achieve non-trivial robustness against multi-step adversaries using adversarial training on two or three step attacks, they are significantly weaker than recent single-step defense methods such as FBF [40] and R-MGM [38]. Thus, we restrict our primary comparisons to the latter defenses which are more robust for a similar computational budget. We use the GAT defense trained on the ResNet-18 architecture for further evaluations in this section.

S6.1 Ablation Experiments

We present ablations on the proposed defense GAT, trained on CIFAR-10 dataset in Table-S3. The architecture of the models is ResNet-18, and the models are trained to be robust under an ℓ_∞ threat model of $8/255$. We present results against PGD-100 step attack and the recently proposed ensemble of attacks, AutoAttack [10]. In order to diversify the attacks generated for GAT training, we switch between standard cross-entropy loss and the proposed GA-CE loss (Algo.-S1, L7) in alternate iterations. However, even without this additional diversification step (Ablation-A1), we observe similar accuracy on AA with merely a marginal drop. We observe that using the original GAMA loss (Eq.1) for both generation of attack and adversarial training does not lead to improved robustness (Ablation-A2). This is because minimization of maximum-margin objective is not suitable for training Deep Neural Networks.

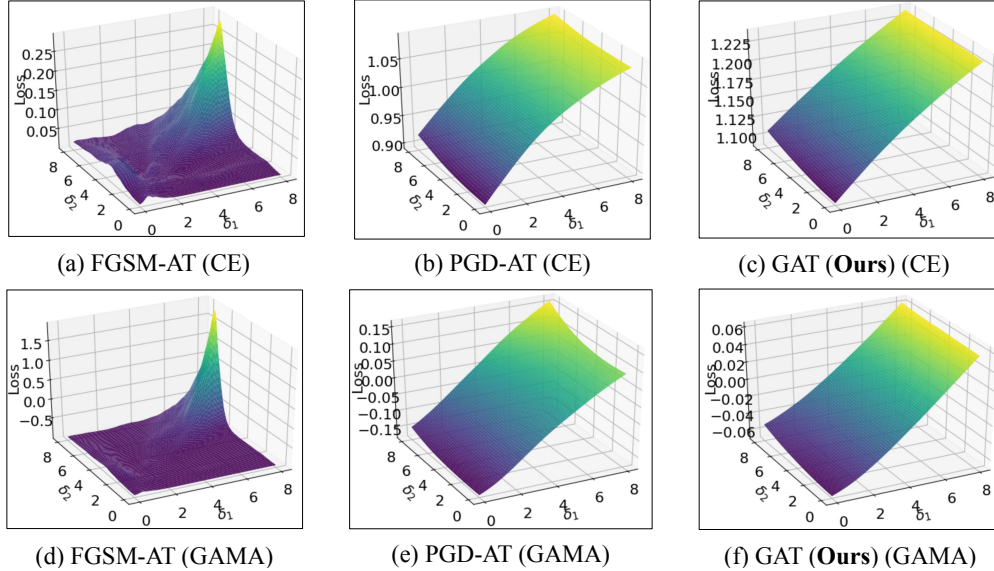


Figure S4: Plot of the loss surface of different models on perturbed images of the form $x^* = x + \delta_1 g + \delta_2 g^\perp$, obtained by varying δ_1 and δ_2 . Here g is the sign of the gradient direction of the cross-entropy loss with respect to the clean image (x) and g^\perp is a direction orthogonal to g .

The proposed defense involves the use of a modified loss function for both attack generation and adversarial training. We perform experiments to evaluate the impact of each of these components individually. The model in Ablation-A3 is trained using GA-CE attack based adversaries. Adversarial training in this experiment is done by minimizing cross-entropy loss on both clean and adversarial samples, in similar vein to R-FGSM adversarial training. While R-FGSM training (Ablation-A4) leads to an improvement over this method, it is still significantly weaker than the proposed defense. Similarly, we find that using the GAT loss for defense alone (Ablation-A5) does not lead to significantly improved robustness. Therefore a combined usage of the loss in both attack generation and adversarial training is crucial for the state-of-the-art results obtained using GAT.

S6.2 Stability of Guided Adversarial Training

In this section, we investigate the stability of the proposed training algorithm on the CIFAR-10 dataset. We train a ResNet-18 model multiple times allowing different random initialisation of network parameters in each run. For each run, we follow the training methodology as outlined in Sections S3.2 and S3.3. We observe that models trained using GAT are very stable; the PGD-100 accuracy obtained over six random reruns are as follows: 52.14, 51.7, 52.02, 52.35, 51.96, 51.74. The low variance (Standard Deviation = 0.224) across multiple runs highlights the stability of the proposed training method. Further, we note that models trained using GAT do not suffer from catastrophic overfitting, as observed in prior works such as FBF [40]. In Fig.S2, we observe that the Cross-Entropy loss on adversaries generated using an FGSM attack is highly similar to the loss on PGD 7-step adversaries throughout the entire training regime, indicating the absence of catastrophic overfitting. We also observe that even the model obtained in the last epoch of training achieves high adversarial accuracy against strong multi-step attacks, in sharp contrast to models obtained towards the end of training using FBF.

S6.3 Loss Surface Plots

To verify the absence of gradient masking, we visualise the loss surface of models trained using the proposed single-step defense GAT, in the neighbourhood of a test data sample. To generate the loss surface, we plot the loss obtained by perturbing the clean sample x along two directions: one along the direction of the gradient of the loss at sample x , and another direction that is orthogonal to the gradient. In Fig.S4 (a), (b) and (c), we plot the standard cross-entropy loss for FGSM-AT, PGD-AT and GAT trained models respectively. We find that FGSM training produces models with significant gradient masking and a convoluted loss surface. On the other hand, for PGD-AT and GAT models, the loss surface is smooth, thereby verifying the absence of gradient masking in the proposed single-step defense. In the second row of Fig.S4, we plot the proposed GAMA loss (Eq.1 of the main paper), which is a combination of the maximum margin loss and the squared ℓ_2 distance between the softmax predictions of the perturbed image and original data sample respectively. The squared ℓ_2 relaxation term is weighted by a constant value of $\lambda = 25$ for obtaining the loss surface plots in Fig.S4 (d), (e) and (f). We again find that the loss surface for the proposed defense GAT is smooth, despite being a single-step

Table S4: **Defenses (ImageNet-100)**: Accuracy (%) of different defenses (rows) trained on ResNet-18 architecture against various ℓ_∞ norm bound (8/255) white-box attacks (columns). The first partition corresponds to single-step defenses, and the second to multi-step defenses. For the Carlini and Wagner (C&W) attack, the Mean- ℓ_2 norm required to achieve high Fooling Rate (FR) is reported. Higher the ℓ_2 norm, better is the robustness.

Method	Clean Acc (%)	FGSM	IFGSM 7-step	Acc (%) on ℓ_∞ attacks			GAMA PGD-100	AA	C & W Mean ℓ_2
				PGD (n-steps) 7	20	500			
Normal	81.44	8.22	0.08	0.06	0.02	0.00	0.00	0.00	0.570
RFGSM-AT [35]	78.46	32.04	23.52	21.64	15.86	13.88	13.38	12.96	2.960
FBF [40]	57.32	36.24	26.92	29.84	28.00	27.22	21.78	20.66	0.737
R-MGM [38]	64.84	40.80	35.18	35.60	32.48	31.68	27.46	27.68	1.636
GAT (Ours)	67.98	45.38	39.66	40.18	38.02	37.46	29.30	28.92	1.499
PGD-AT [25]	68.62	43.04	40.00	39.64	37.20	36.56	32.24	32.98	1.550
TRADES [43]	62.88	40.46	38.52	38.44	37.34	37.24	31.44	31.66	1.360

Table S5: **Defenses (MNIST)**: Accuracy (%) of different defenses (rows) trained on M-LeNet architecture (Table-S1) against various ℓ_∞ norm bound (0.3) white-box attacks (columns). The first partition corresponds to single-step defenses, and the second to multi-step defenses. For the Carlini and Wagner (C&W) attack, the Mean- ℓ_2 norm required to achieve high Fooling Rate (FR) is reported. Higher the ℓ_2 norm, better is the robustness.

Method	Clean Acc (%)	FGSM	IFGSM 40-step	Acc (%) on ℓ_∞ attacks			GAMA PGD-100	AA	C & W Mean ℓ_2
				PGD (n-steps) 40	100	500			
Normal	99.20	16.59	0.48	0.02	0.00	0.00	0.00	0.00	1.42
RFGSM-AT [35]	99.37	92.44	89.47	90.24	85.85	85.32	83.64	82.28	2.19
FBF [40]	99.30	97.47	94.53	94.85	92.35	91.37	87.27	79.02	1.91
R-MGM [38]	99.04	96.35	93.09	93.06	90.96	90.56	88.13	86.21	2.31
GAT (Ours)	99.37	97.11	95.61	96.11	94.58	94.44	92.96	90.62	2.30
PGD-AT [25]	99.27	96.27	94.91	95.53	94.14	93.98	92.80	91.81	2.63
TRADES [43]	99.32	96.08	94.86	95.26	93.52	93.40	92.74	92.19	2.53

defense method. We further note that the GAMA loss surface is smoother than the cross-entropy loss surface for all three models, specifically for the FGSM model. This helps explain why the proposed GAMA attack is more effective than the standard maximisation of the cross-entropy loss.

S6.4 Performance against White-Box attacks

The results on white-box adversarial attacks for ImageNet-100 and MNIST datasets are presented in Table-S4 and Table-S5 respectively. On both datasets, we observe significant improvement in robustness with the proposed approach when compared to existing single-step adversarial training methods. We also note that the robustness achieved is comparable to the multi-step adversarial training methods, TRADES and PGD-AT, presented in the second partition of both tables.

We also evaluate all the defenses on MNIST and ImageNet-100 datasets against the proposed GAMA-PGD attack. The proposed defense is stronger compared to all other defenses even on the GAMA-PGD 100-step attack. The proposed GAMA-PGD attack is notably stronger than all the single attacks considered here. We note that for ImageNet-100 dataset, a single run of the GAMA-PGD attack is comparable to the AA attack, which is an ensemble of multiple attacks with five random restarts each. In particular, the GAMA-PGD attack is significantly stronger than the APGD-CE, APGD-DLR, FAB and Square attacks that constitute the AA ensemble attack. For MNIST dataset, GAMA-PGD is comparable to AA on some defenses and significantly weaker than AA on few others. This is primarily because one of the attacks in the AA ensemble is the Square attack, which is a query based attack. This is a gradient-free attack and is therefore significantly stronger than gradient-based attacks in cases where the loss surface is complex, leading to masking of the true gradient direction.

While the defense is trained to be robust against ℓ_∞ norm bound perturbations, we find that the robustness to the ℓ_2 norm based Carlini & Wagner (C&W) attack [5] is comparable to other ℓ_∞ norm based adversarial training methods. We also evaluate the proposed method (GAT with ResNet-18 architecture) on the DDN attack [30] for CIFAR-10 dataset, and obtain a mean ℓ_2 norm of 0.805 for adversarial perturbations, compared to 0.762 as

Table S6: Prediction accuracy (%) of our model (GAT) in various targeted and untargeted White-Box attack settings. Among the targeted attacks, we consider 1000-step Least Likely attack and 1000-step Random target attack. In the second partition, worst case robustness against multiple random restarts is reported. We consider a 1000-sample subset of CIFAR-10 and ImageNet-100 datasets for the random restarts experiments.

Attack	CIFAR-10		ImageNet-100		MNIST	
	500-step	1000-step	500-step	1000-step	500-step	1000-step
PGD-Targeted (Least Likely class)	79.50	79.50	66.12	66.02	99.03	99.03
PGD-Targeted (Random class)	74.56	74.37	63.80	64.10	98.86	98.84
PGD-Untargeted	53.04	53.04	37.52	37.52	94.37	94.37
	1-RR	1000-RR	1-RR	500-RR	1-RR	1000-RR
PGD 50-step, r-RR	53.20	52.10	38.70	38.30	95.46	92.20

Table S7: Prediction accuracy (%) of different defenses in **FGSM Black-Box attack** setting. Source model for attack is specified in the column headings. Target model is specified in each row.

Method	CIFAR-10			ImageNet-100			MNIST		
	Clean	VGG11	ResNet18	Clean	AlexNet	ResNet18	Clean	BB-MNIST	M-LeNet
Normal	92.30	37.09	15.98	81.44	63.82	8.22	99.05	38.62	16.58
RFGSM-AT [35]	89.66	82.62	85.74	78.46	74.82	74.18	99.37	93.79	92.44
FBF [40]	82.83	78.19	80.41	57.32	56.12	56.22	99.30	95.56	95.19
R-MGM [38]	82.29	78.18	79.99	64.84	63.26	63.60	99.04	95.52	95.19
GAT (Ours)	80.49	76.95	78.54	67.98	65.94	65.98	99.37	96.51	96.49
PGD-AT [25]	82.67	78.91	80.53	68.62	67.02	67.34	99.27	95.68	96.27
TRADES [43]	81.73	78.28	79.65	62.88	61.42	61.42	99.32	96.49	96.08

obtained with the Carlini and Wagner (C&W) ℓ_2 attack, indicating that the latter is stronger. Thus, we primarily utilise the C&W attack for the evaluation of defense models on ℓ_2 norm-constrained adversaries.

We evaluate our proposed approach on 1000-step PGD targeted and untargeted attacks. The results of these experiments are presented in Table-S6. Targeted attacks are weaker than untargeted attacks, thereby resulting in a higher accuracy. We note that the attack converges within 1000-steps based on the observation that drop in accuracy between 500-step attack and 1000-step attack is marginal.

We present the worst-case accuracy of GAT-trained models across multiple random restarts of PGD 50-step attack in the second partition of Table-S6. The results are shown on a 1000-image subset of CIFAR-10 and ImageNet-100 test sets and on the full MNIST test set. In order to find the worst-case accuracy, we continue restarts until accuracy stabilizes. We note that the robustness of the proposed defense is not broken by attacks using random restarts, thereby demonstrating the absence of gradient masking.

Table S8: Prediction accuracy (%) of different models in **PGD-7 step Black-Box attack** setting. Source model for attack is specified in the column headings. Target model is specified in each row.

Method	CIFAR-10			ImageNet-100			MNIST		
	Clean	VGG11	ResNet18	Clean	AlexNet	ResNet18	Clean	BB-MNIST	M-LeNet
Normal	92.30	20.88	0.00	81.44	72.48	0.04	99.05	8.03	0.01
RFGSM-AT [35]	89.66	84.96	87.36	78.46	76.58	76.24	99.37	94.93	89.47
FBF [40]	82.83	79.62	81.32	57.32	56.66	56.84	99.30	96.53	96.51
R-MGM [38]	82.29	79.33	80.92	64.84	63.88	64.20	99.04	96.03	96.28
GAT (Ours)	80.49	77.88	79.25	67.98	66.58	66.80	99.37	97.25	97.52
PGD-AT [25]	82.67	79.68	81.26	68.62	67.66	67.90	99.27	96.46	94.91
TRADES [43]	81.73	79.04	80.22	62.88	62.28	62.26	99.32	96.98	94.86

Table S9: Prediction accuracy (%) of different defenses against the query based Black Box attack, Square.

Method	CIFAR-10		ImageNet-100		MNIST	
	Clean	Square	Clean	Square	Clean	Square
Normal	92.30	0.16	81.44	0.66	99.05	0.02
RFSGM-AT [35]	89.66	43.01	78.44	41.60	99.37	84.13
FBF [40]	82.83	52.46	57.32	28.38	99.30	79.66
R-MGM [38]	82.29	52.87	64.82	38.34	99.04	88.89
GAT (Ours)	80.49	53.62	67.98	39.06	99.37	91.03
PGD-AT [25]	82.67	52.64	68.60	45.50	99.27	91.99
TRADES [43]	81.73	54.87	62.86	40.30	99.32	92.60

Table S10: Prediction accuracy (%) of our proposed single-step defense GAT against adaptive attacks constructed using diverse settings (rows).

λ_{attack}	Decay Iterations	CIFAR-10		ImageNet-100		MNIST	
		GA-CE	GAMA	GA-CE	GAMA	GA-CE	GAMA
0	no decay	52.93	48.40	36.66	30.14	93.22	93.06
$\lambda_{defense,init}$	no decay	52.83	49.78	35.76	32.80	93.07	93.20
$\lambda_{defense,final}$	no decay	53.63	51.74	35.64	35.18	93.09	93.15
50	25	52.80	47.76	36.58	29.24	93.02	93.00
100	25	52.75	47.92	36.66	29.34	93.13	93.05
50	50	52.73	47.88	36.56	29.40	93.20	93.02
100	50	52.84	47.97	36.58	29.30	93.23	93.11
50	100	53.00	50.64	36.58	32.22	93.19	93.15
100	100	53.34	51.68	35.52	33.54	93.39	93.35

S6.5 Performance against Black-Box and gradient-free attacks

The results on FGSM and PGD 7-step Black-box attacks are presented in Table-S7 and Table-S8 respectively. We consider two sources for Black-box attacks; the first with the same architecture as the source model, and the second with a different architecture. Across all three datasets, accuracy on black-box attacks closely tracks the accuracy on clean samples, and is higher than that of white-box attacks. This confirms that there is no issue of gradient masking in the proposed model, which could potentially generate weaker adversaries, thereby creating a false sense of robustness.

We present results on the query-based black-box attack, Square [2] in Table-S9. We note that across most defenses, this attack is weaker than PGD-500 step attack for CIFAR-10 and ImageNet-100, whereas it is stronger than the same for MNIST. The proposed defense achieves improved robustness compared to existing single-step adversarial defenses on MNIST and CIFAR-10 datasets. For Imagenet-100, although R-FGSM achieves better accuracy, it is significantly more susceptible to white-box attacks presented in Table-S4. The performance of the proposed single-step defense GAT against the strong query based Square attack shows that the robustness of the proposed defense is not a result of gradient masking.

Further, we evaluate the proposed defense against SPSA [37], a gradient-free attack that utilises a numerical approximation of gradients by sampling function values along random directions. We use the following standard hyperparameters for attack generation using SPSA: learning rate = 0.01, $\delta = 0.01$, number of iterations = 100 and number of samples to approximate the average gradient = 128. On the CIFAR-10 dataset, the proposed single-step GAT defense with ResNet-18 architecture achieves 56.59% accuracy against SPSA, compared to 53.62% on the Square attack. Since the Square attack is stronger than SPSA, we use the former to present gradient-free attack evaluation of all defense methods in Table-S9.

S6.6 Performance Against Adaptive Adversaries

Since we consider the framework of worst-case adversarial robustness, we assume that the adversary has complete knowledge of the defense mechanism employed. Thus, it is crucial to evaluate our model on adaptive adversaries as well [6]. We consider strong multi-step PGD attacks, where the adversary attempts to maximise the proposed loss at each step. More precisely, the adversaries are generated using the proposed GA-CE or GAMA loss, where the first term is either cross-entropy loss or maximum margin loss, and the second term

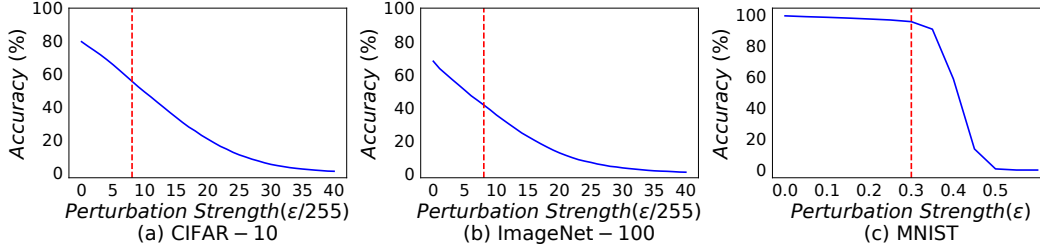


Figure S5: Plot showing the variation of accuracy on 7-step PGD samples across the magnitude of perturbation, ϵ for the proposed single-step defense, GAT. Accuracy goes to zero for large ϵ across all datasets, indicating the absence of gradient masking.

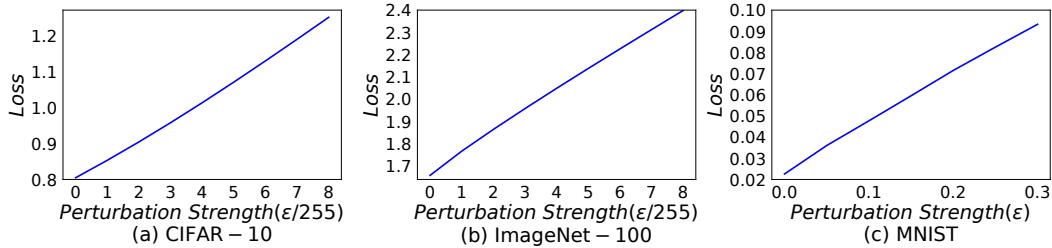


Figure S6: Plot showing the variation of loss on FGSM samples across the magnitude of perturbation, ϵ for the proposed single-step defense, GAT. Loss increases monotonically with an increase in ϵ across all datasets, indicating the absence of gradient masking.

is the squared ℓ_2 distance between the softmax outputs of the original clean image and the adversarial sample generated in the previous step. We evaluate the proposed defense against diverse settings of the attack, using the cross-entropy loss in one case (GA-CE) and maximum-margin loss in the second (GAMA). We present our experiments and results in Table-S10. We consider a case without λ decay over iterations, where the λ used in the attack (λ_{attack}) is same as the λ used in defense ($\lambda_{defense,init}$). We also consider a case where $\lambda_{attack} = \lambda_{defense,final}$ which is the same as $\lambda_{defense,init}$ multiplied by the step-up factor. In general, the cross-entropy based attack is weaker than the margin based attack. The adaptive attacks are significantly stronger than standard PGD-based attacks. However, they are not as strong as the AutoAttack (AA). We note that it is not fair to compare the strength of a single attack with an ensemble of attacks, which declares a given data sample to be robust only if it passes all the attacks in the ensemble. Therefore, although we generate strong adaptive attacks, robustness of the proposed approach does not deteriorate further compared to AutoAttack.

S6.7 Sanity checks to ensure absence of gradient masking

We observe from the above experiments that iterative attacks are stronger than single-step attacks (Table-2 in the main paper, Tables-S4 and S5). Furthermore, white-box attacks are stronger than black-box attacks (Table-2 in the main paper, Tables-S4, S5, S7 and S8). In the plot shown in Fig.S5, we increase the value of ϵ and observe that unbounded attacks are able to reach 100% attack success rate for all datasets. Also, as shown in Fig.S6, the loss monotonically increases with an increase in the perturbation size of the FGSM attack. These tests confirm that the model is truly robust, and the observed robustness is not a result of gradient masking.